the distinct asymmetry at 0 deg, and the gradual approach to symmetry at 90 deg.

In summary, a simple closed-form model has been developed for a three-dimensional vacuum plume from a scarfed nozzle. The model is convenient to use and is adaptable to hand calculators or for onboard algorithms. It is based upon satisfying mass and momentum conservation, while assuming a maximum density along the skewed thrust vector, and an expansion at the nozzle lip based on the local flow conditions around the nozzle periphery. The model can use either analytical or test-determined thrust vector coefficients. For zero scarf angles, the model collapses to an axisymmetric form which is applicable up to the inviscid plume boundary angle.

References

[1] Boynton, F. P., "Highly Underexpanded Jet Structure: Exact and Approximate Calculations," *AIAA Journal*, Vol. 5, Sept. 1967, pp. 1703-1704.

[2] Karydas, A. I. and Kato, H. T., "An Approximate Method for Calculating the Flow Field of a Rocket Exhausting into a Vacuum," Aeronutronics TN No. 24, June 15, 1964.

Singular Propagation Behavior of Cracks in Stiffened Cylindrical Shells

Chang Shangchow*
Northwestern Polytechnical University, Xian, China

Introduction

THIS Note discussed two new findings in crack propagation behavior: namely, the adverse effect of stiffeners on the fracture strength of, and the biased fatigue crack propagation in stiffened cracked cylindrical shells. The former implies that the fracture strength of a stiffened cracked shell can be inferior to that of a similar but unstiffened one under certain conditions, while the latter refers to the sheer unsymmetrical fatigue crack propagation taking place from a symmetrical stiffened cracked shell under symmetrical loading conditions prior to and during the early stage of the crack propagation. These manifestations of crack propagation behavior are all seemingly abnormal and may be called singular. In subsequent sections, we will first describe the phenomenon of singular behavior, together with related testing data. Then an approximate engineering analysis of the stress intensity factors in stiffened cracked shells will be given as evidence that the singular behavior really results from the interaction between stiffeners and cracks in shells. This interaction, in general, is complicated and must be treated carefully in the design of shell-like structural components, such as aircraft pressure cabins, under the concept of damage tolerance.

Testing Data and Phenomena

Singular propagation behavior has been observed during the fracture and fatigue crack propagation tests on stiffened, longitudinally cracked circular cylindrical shell specimens. All of the shells and the circumferential ring-shaped stiffeners were fabricated from 1-mm thick, 2024-T3 aluminum alloy rolled plates. Three types of final specimen configurations are shown in Fig. 1. The stiffeners are attached to the shells' outer surfaces by riveting. Prior to testing, a thorough longitudinal crack symmetrical to the center section of the shell was precracked into each specimen. A uniform, monotonically increasing (or fluctuating) hydraulic pressure was applied on the inner surface of a specimen during fracture (or fatigue crack propagation) testing.

The adverse effect of stiffeners on the fracture strength of cracked shells presented itself in the fracture tests on double-stiffened specimens, as if the crack length is within a definite range, the fracture strength of double-stiffened cracked shells will be inferior rather than superior to that of similar unstiffened shells. This conclusion is supported by the testing evidence of the average value of the burst pressure in fracture tests for double-stiffened specimens having an initial crack of 60 mm in length, 5.66 normal atm, and a higher average value of 6.25 normal atm for similar unstiffened specimens. Also, using the well-known Paris-Foreman law,

$$\frac{da}{dN} = \frac{C_1(\Delta K)^m}{(1-K_{\min}/K_{\max})K_c - \Delta K} \tag{1}$$

the testing data obtained from the fatigue crack propagation tests on various specimens have been processed statistically by the least-squares technique and the final results are $C_1 = 3.31 \times 10^{-12}$, $m = 5.35$ for unstiffened specimens, and $C_1 = 3.98 \times 10^{-12}$, $m = 5.35$ for double-stiffened shell specimens. The data demonstrate clearly that the fatigue crack propagation resistance of double-stiffened specimens is weaker than that of similar unstiffened specimens, in agreement with the results of fracture tests. On these grounds it is recognized that the adverse effect does exist.

The biased fatigue crack propagation behavior was observed in fatigue crack propagation tests on single-stiffened cracked shell specimens. It appeared that during the early stage of fatigue crack growth, two tips of the crack (having a initial length of 40 mm) propagated essentially symmetrically, i.e., both tips gained almost the same crack length increment when a definite number of loading cycles had been carried out. This symmetrical manner of crack propagation appeared normal since, prior to the initiation of fatigue crack growth, all the testing conditions were symmetric to the central stiffener and the external load was a hydraulic pressure (fluctulating between 2-10 normal atm) applied uniformly over the inner surface of the shell. However, whenever the one-sided crack length increment reached about 8 mm, one of the tips ceased growing, while the other one continued its course until the one-sided rapid crack propagation took place. At first it was considered that one might attribute the biased crack propagation to some veiled unsymmetrical factors involved in the testing conditions, and a number of measures had been taken to improve the symmetry of the specimen and loading in the testing procedure. Nevertheless, the biased crack propagation presented itself repeatedly. In addition, similarly biased crack propagation was observed in fracture tests of specimens of the same type. During the initial stage of stable

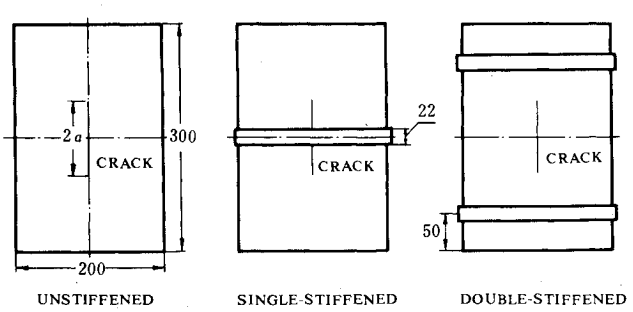

Fig. 1 Specimen configurations (units in millimeters).

Received Dec. 30, 1982; revision received July 11, 1983.

*Associate Professor, Department of Aircraft Engineering.

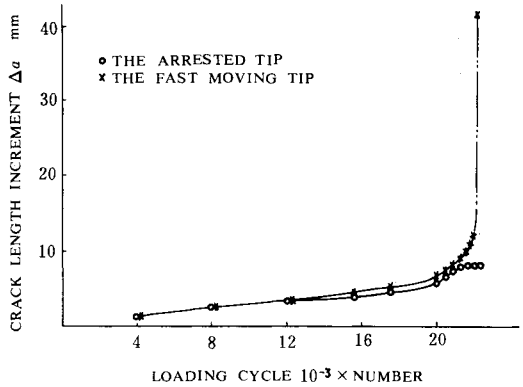

Fig. 2 Testing data curves of fatigue crack propagation test on a single-stiffened specimen.

crack growth, both tips propagated in a similar manner. However, as the test continued, one of the tips arrested and the final failure always resulted from one-sided rapid crack propagation. Therefore, it is concluded that the phenomenon is not probable, but regular.

One of the relating crack length increment vs cycle number diagrams for two tips of a crack in a specimen is reproduced in Fig. 2 to demonstrate the phenomenon of biased fatigue crack propagation.

Analysis and Explanation

In this section a possible explanation for the singular crack propagation behavior, based on an approximate engineering analysis of stress intensity factors in stiffened cracked cylindrical shells, will be given to show that the singular behavior can be recognized as the necessary outgrowth of complicated interactions between stiffeners and cracks in shell structures.

Unstiffened Cracked Shell

Consider an unstiffened shell with a longitudinal crack of length $2a$ under a uniform internal pressure p. For the mere purpose of determining stress intensity factors at the crack tips, by a simple argument of superposition frequently used in fracture mechanics, it is easily seen that the original problem can be reduced to that of a similar cylindrical shell whose inner surface is free from any external load while the crack surfaces are subject to a uniform compressive stress $\sigma_0 = -pR/B$, where R and B are the radius and thickness of the shell, respectively.† The stress intensity factor in the reduced problem is available and can be expressed as

$$K_I = A\sigma_0\sqrt{\pi a}$$

where A is a correction factor, depending on the material and geometry of the shell and can be found in Ref. 1.

Single-Stiffened Cracked Shell

Now consider a single-stiffened cracked shell under the action of a uniform internal pressure p. Evidently in this case, in addition to the internal pressure, the shell itself is subject to a pair of additional external loads—the radial compressive and circumferential shearing forces acting on it by the stiffener. Again, with the use of the superposition argument, the stress intensity factor determination problem of a single-stiffened cracked shell under the action of a uniform pressure p over its inner surface can be replaced by that of a similar shell subjected only to some normal stress σ_I on its crack surfaces, where $-\sigma_I$ represents the normal stress that should occur on the crack surfaces to make the crack fully closed under the combined action of $-\sigma_I$ and p. Using the theory of thin shells,[2] the expression for σ_I can be written as

$$\sigma_I = \sigma_0 + \sigma_I' \equiv -\frac{pR}{B} + \frac{EQ}{8\beta^3 RD} e^{-\beta x}(\cos\beta x + \sin\beta x)$$

$$\beta = \left[\frac{3(1-\nu^2)}{R^2B^2}\right]^{1/4}, \qquad D = \frac{EB^3}{12(1-\nu^2)} \tag{2}$$

where Q is the radial force in unit circumferential length exerted on the shell by the stiffener, ν the Poisson's ratio of the shell's material, and x the coordinate of the longitudinal axis of the shell with the origin located at the stiffener-attaching section.

It is evident that the term σ_I' in Eq. (2) represents the effect of the stiffener on the stress intensity factor and fracture strength of the single-stiffened cracked shell. Ths effect is due mainly to the radial compressive force acting on the shell by the stiffener and may be called the first effect of the stiffener on the fracture strength of the shell. Note that as x increases, σ_I' changes its sign from positive (tensile) to negative (compressive). Incidentally, no such effect is present in the corresponding case of a cracked plate stiffened by a single stiffener.

The circumferential shearing force acting on the shell by the stiffener provides the second effect of the stiffener on the stress intensity factor and fracture strength of the shell. This effect is also present in the corresponding case of stiffened plates, and for a single-stiffened cracked plate under uniform tension σ it is usually manifested in terms of coefficient C in the stress intensity factor computation formula

$$K_I = C\sigma\sqrt{\pi a}, \qquad C \le 1 \tag{3}$$

This effect is rather difficult to evaluate in shell structures. However, the general trend of the C-a curve must remain unchanged; namely, for $a \to 0$ and ∞, $C \to 1$; and there is a point (say point M) somewhere near the stiffener at which C reaches a minimum.

The foregoing approximate analysis can be applied essentially similar to double-stiffened cracked shells.

Explanation

Now the approximate analysis is utilized to give an explanation of the singular propagation behavior as follows. In the case of a double-stiffened configuration, unless the crack tips approach the immediate vicinity of the stiffeners, the effect represented by coefficient C in Eq. (3) is very weak and the additional normal stress σ_I' on the crack surface is negative. Hence, compared with the unstiffened configuration, higher values of stress intensity factors will result, together with a lower burst pressure and a shorter fatigue crack propagation life.

For the single-stiffened configuration, at the initial stage of fatigue crack propagation the two tips propagate at essentially the same speed. If one of the two tips moves a little faster, it will suffer a greater retarding action represented by coefficient C which has a minimum at point M some distance away from the stiffener. However, one of the tips first must reach and pass point M and move faster and faster, due to the combined effect of σ_I' and C. As the tip advances, C increases monotonously and σ_I' changes from positive to negative. The longer crack length and the wider crack opening displacement created by the fast-moving tip can bring about a greater circumferential shearing force on the shell. However, this retarding force is too far for the hurriedly advancing tip to have any actual influence on it, while the lagged one is under its full effect and cannot move any more even when the fast moving tip has vanished in the rapid crack propagation.

†Some minor bending stress may also be present on the crack surfaces, but, in general, it is too small in magnitude compared with σ_0 to be included in this approximate analysis.

Acknowledgment

The author is grateful to Mr. Zhang Bao-fa and Mr. Liu Xue-hui for their collaboration in the testing work reported in this Note.

References

[1]Erdogan, F., "Crack Problems in Cylindrical and Spherical Shells," *Mechanics of Fracture 3*, Noordhoff, Leyden, 1977, pp. 161-198.

[2]Timoshenko, S. and Woinowsky-Krieger, S., *Theory of Plates and Shells*, McGraw-Hill Book Co., New York, 1959.

Derivation and Significance of Second-Order Modal Design Sensitivities

J. A. Brandon*
University of Manchester
Institute of Science and Technology
Manchester, England

Introduction

CONSIDER the eigenproblem

$$(\lambda \underline{\underline{A}} + \underline{\underline{B}})\underline{x} = 0 \tag{1}$$

having eigenvalues λ_i and eigenvectors $\underline{\phi}_i$. Such a problem is typical either of a conservative dynamical system or a viscously damped system reduced to its Duncan form, i.e.,

$$\lambda \begin{pmatrix} \underline{\underline{0}} & \underline{\underline{M}} \\ \underline{\underline{M}} & \underline{\underline{C}} \end{pmatrix} \begin{pmatrix} \lambda \underline{x} \\ \underline{x} \end{pmatrix} + \begin{pmatrix} -\underline{\underline{M}} & \underline{\underline{0}} \\ \underline{\underline{0}} & \underline{\underline{K}} \end{pmatrix} \begin{pmatrix} \lambda \underline{x} \\ \underline{x} \end{pmatrix} = 0 \tag{2}$$

If the system is considered to be unsatisfactory in some way, e.g., a natural frequency to the system coinciding with a constant shaft speed, then it is of interest to find the design change which will give maximum benefit with minimum disturbance to the system. This may be quantified in terms of design sensitivities of the structure.

Fox and Kapoor[1] derived an expression for the sensitivity of an eigenvalue for self-adjoint systems (i.e., where the left and right eigenvectors are simple transposes, typical of conservative systems and Duncan forms). Garg[2] extended this result to apply to non-self-adjoint systems (e.g., where dissipative and gyroscopic effects are present). The analysis for eigenvectors was presented by Plaut and Huseyin[3] for the general case. Most recently, Nelson[4] has provided an alternative approach to eigenvector sensitivity. The sensitivities derived by all of the above methods are expressed in the form of (first) derivatives and, hence are properties local to the original solution of the system. In a recent paper by Vanhonacker,[5] there is a clear implication that these first derivatives may be extrapolated for gross system changes. Clearly this assumption can be valid only if the value of the second derivative is negligible.

Received Feb. 26, 1982; revision received May 17, 1983.

*Research Student, Mechanical Engineering Department, Manufacturing and Machine Tools Division; currently Lecturer in Manufacturing Systems, University of Wales Institute of Science and Technology, Cardiff, Wales.

A perturbation approach similar to that used by Lancaster[6] will be used here to derive the second-order sensitivities (second derivatives) from first principles. It will be possible then to quantify under what conditions the assumptions of Vanhonacker are valid. Only the symmetrical (and, hence, self-adjoint) case will be considered, but the results will readily generalize to non-self-adjoint systems.

First- and Second-Order Perturbations

Consider a small variation $\epsilon \underline{\underline{Q}}$ in the right-hand side of Eq. (1). Let the eigenvalues of Eq. (1) be $\lambda_i, \underline{\phi}_i$ $(1 \le i \le n)$. The eigenvalues of the perturbed problem

$$(\lambda \underline{\underline{A}} + \underline{\underline{B}})\underline{x} = \epsilon \underline{\underline{Q}} \underline{x} \tag{3}$$

are denoted by λ_i^p, $\underline{\phi}_i^p$.

The characteristic equation (3) is polynomial in both λ and ϵ and hence we may express the perturbed eigenvalue as a power series in ϵ.

$$\lambda_i^p = \lambda_i + \eta \epsilon + \zeta_i \epsilon^2 + \ldots \tag{4}$$

and as a consequence of the Cayley-Hamilton theorem we may express the eigenvectors in a similar way

$$\underline{\phi}_i^p = \underline{\phi}_i + \underline{\mu}_i \epsilon + \underline{\nu}_j \epsilon^2 + \ldots \tag{5}$$

Because we are free to scale $\underline{\phi}_i^p$ and $\underline{\phi}_i$, we may make $\underline{\mu}_i$ and $\underline{\nu}_j \underline{\underline{A}}$ orthogonal to $\underline{\phi}_i$ following Lancaster, i.e.,

$$\underline{\mu}_i^T \underline{\underline{A}} \underline{\phi}_i = \underline{\nu}_j^T \underline{\underline{A}} \underline{\phi}_i = 0 \tag{6}$$

Substituting Eqs. (4) and (5) into Eq. (3) and neglecting terms greater than $O(\epsilon^2)$

$$[(\lambda_i + \eta_i \epsilon + \zeta_i \epsilon^2)\underline{\underline{A}} + \underline{\underline{B}}](\underline{\phi}_i + \underline{\mu}_i \epsilon + \underline{\nu}_j \epsilon^2) = \epsilon \underline{\underline{Q}}(\underline{\phi}_i + \underline{\mu}_i \epsilon + \underline{\nu}_j \epsilon^2) \tag{7}$$

Now compare the coefficients in successive powers of ϵ

$$\epsilon^0: \quad (\lambda_i \underline{\underline{A}} + \underline{\underline{B}})\underline{\phi}_i = \underline{0}$$

$$\epsilon^1: \quad \eta_i \underline{\underline{A}} \underline{\phi}_i + \lambda_i \underline{\underline{A}} \underline{\mu}_i + \underline{\underline{B}} \underline{\mu}_i = \underline{\underline{Q}} \underline{\phi}_i \tag{8}$$

$$\epsilon^2: \quad \zeta_i \underline{\underline{A}} \underline{\phi}_i + \eta_i \underline{\underline{A}} \underline{\mu}_i + \lambda_i \underline{\underline{A}} \underline{\nu}_i + \underline{\underline{B}} \underline{\nu}_i = \underline{\underline{Q}} \underline{\nu}_i \tag{9}$$

We may restate Eq. (6) in the form

$$\underline{\mu}_i = \sum_{\substack{j=1 \\ j \ne i}}^{n} \alpha_{i,j} \underline{\phi}_j \tag{10}$$

and

$$\underline{\nu}_i = \sum_{\substack{j=1 \\ j \ne i}}^{n} \beta_{i,j} \underline{\phi}_j \tag{11}$$

because of the well-known orthogonality condition

$$\underline{\phi}_j^T \underline{\underline{A}} \underline{\phi}_i = 0, \qquad j \ne i \tag{12}$$

Premultiplying Eq. (8) by $\underline{\phi}_i$ and taking into account the orthogonality conditions

$$\eta_i = \frac{\underline{\phi}_i^T \underline{\underline{Q}} \underline{\phi}_i}{\underline{\phi}_i^T \underline{\underline{A}} \underline{\phi}_i} \tag{13}$$